

Chemistry and structure analysis in the $\text{Li}_{4+x}\text{B}_x\text{Si}_{1-x}\text{O}_4$ solid solution

C. Masquelier¹, H. Kageyama, T. Takeuchi, Y. Saito, O. Nakamura

Osaka National Research Institute, AIST, 1-8-31, Midorigaoka, Ikeda, Osaka 563, Japan

Abstract

The crystal chemistry of the Li_4SiO_4 -based solid solution $\text{Li}_{4+x}\text{B}_x\text{Si}_{1-x}\text{O}_4$ is presented. Synthesis was carried out using $\text{LiOH}\cdot\text{H}_2\text{O}$ or Li_2CO_3 as starting materials. Stoichiometric mixtures with $0 \leq x \leq 0.7$ were fired at temperatures ranging from 670 to 850 °C. A CO_2 -free atmosphere is required to avoid the presence of Li_2CO_3 in the remaining solid. Small amounts of LiOH are detected in samples prepared from $\text{LiOH}\cdot\text{H}_2\text{O}$. The solubility of boron in the solid solution is also discussed in terms of crystal structure analysis. The lithium insertion is accompanied with a continuous slight increase in the unit-cell volume. $x=0.5$ is the maximum composition above which Li^+ insertion should be accompanied with a modification of the Li_4SiO_4 -based structure.

Keywords: Solid solution; Lithium; Boron; Silicon oxide; Crystal structure; Lithium orthosilicates

1. Introduction

Over the past twenty years, Li_4SiO_4 -based materials have been extensively studied as possible solid electrolytes for high-temperature solid-state devices. Li_4SiO_4 itself is a poor ionic conductor ($\sigma_{300^\circ\text{C}} = 10^{-5} \text{ S cm}^{-1}$) [1,2]. Several works have, however, demonstrated that the ionic conductivity of this family of orthosilicates can be greatly enhanced by substituting lithium and/or silicon for trivalent cations M^{3+} ($\text{M} = \text{Al}, \text{Ga}, \text{B}$) [3–7]. At this point, two major substitution mechanisms should be considered: (i) the creation of additional lithium vacancies or (ii) the introduction of extra Li ions in the structure.

Substitution on to the lithium sites leads to $\text{Li}_{4-3y}\text{M}_y\text{SiO}_4$ compositions on the join Li_4SiO_4 – LiM_3SiO_4 where $y < 0.6$ and $y < 0.25$ for $\text{M} = \text{Al}$ and Ga , respectively [3,4].

Substitution on to the silicon sites leads to $\text{Li}_{4+x}\text{M}_x\text{Si}_{1-x}\text{O}_4$ compositions on the join Li_4SiO_4 – Li_5MO_4 . The Li_4SiO_4 -based $\text{Li}_{4+x}\text{M}_x\text{Si}_{1-x}\text{O}_4$ solid solutions were found to extend up to $x=0.4$ and $x=0.3$ for $\text{M} = \text{Al}$ and Ga , respectively [5,6]. Recently, Saito et al. [7] also studied the boron-substituted solid solution

and found a surprisingly high solubility limit of $x=0.7$, as well as a very particular evolution of the b -lattice parameter with increasing x . Additionally, they report detecting the systematic presence of Li_2CO_3 impurity in the solids obtained from starting compositions in which $x > 0.5$.

Recent works have been devoted to determine the crystal structures of several compositions within those solid solutions which were expected to provide a useful insight into their high cation-transport properties [8,9]. Several explanations have been proposed to account for this phenomenon. These include such hypotheses as an increase in the charge-carriers concentration [10], an increase in the hopping rate [7], or the presence of impurity phases such as LiOH , which was found to coexist with lithium silicoaluminates $\text{Li}_{4+x}\text{Al}_x\text{Si}_{1-x}\text{O}_4$, for $x=0.2$ and $x=0.3$ [11].

Thus, we present in this paper our recent re-investigation of the boron-substituted solid solution. We describe the different routes investigated for the synthesis. Additional attention is also given to studying the effect of the surrounding atmosphere on impurity formation during the firing. Previously reported crystal structures of Li_4SiO_4 [12–14] are also closely examined; we conclude that there is a maximum composition in the solid solution of $x=0.5$, above which the introduction of extra lithium ions should be accompanied with a change in the Li_4SiO_4 structure.

¹ New address: University of Texas at Austin, ETC 9.102, Austin, TX 78712-1084, USA.

2. Experimental

$\text{Li}_{4+x}\text{B}_x\text{Si}_{1-x}\text{O}_4$ compounds were prepared from reagent grade H_3BO_3 , SiO_2 and either $\text{LiOH}\cdot\text{H}_2\text{O}$ or Li_2CO_3 . Intimate stoichiometric mixtures were placed in an Al_2O_3 crucible or a gold foil boat and fired at alternate intervals between 500 and 850 °C. Platinum crucibles could not be used as they were systematically attacked by Li_2O , resulting in a significant formation of yellowish green Li_2PtO_3 powder. The samples obtained were stored in an argon-filled glove box to avoid hydration and carbonation. The different phases occurring in the samples were identified by their X-ray diffraction (XRD) patterns, recorded on a Rigaku Rotating Anode diffractometer (Cu K α). The $\text{Li}_{4+x}\text{B}_x\text{Si}_{1-x}\text{O}_4$ compounds' patterns were indexed using the Vollekle's unit cell (monoclinic, space group $P2_1/m$) [12]. For precise lattice parameters determinations, the d -spacing values were corrected from systematic deviation by using silicon as an internal standard. Thermal gravimetry (TG) and differential thermal analysis (DTA) experiments were performed on a Rigaku-TG8101D thermal analyzer in an ambient atmosphere. Samples of about 30 mg placed in golden crucibles were heated to $T_{\text{max}}=750$ °C at a heating rate of 10 °C/min.

3. Chemical syntheses

Our first determination was that the atmosphere in which the samples were fired had a major influence on impurity formation, particularly for lithium-rich compositions.

3.1. Synthesis in an ambient atmosphere

Li_4SiO_4 was obtained from a stoichiometric mixture of SiO_2 and $\text{LiOH}\cdot\text{H}_2\text{O}$. In the first stage, the mixture was slowly heated to $T=500$ °C to remove H_2O , which occurs in two steps as demonstrated by DTA and TG experiments (Fig. 1). Similar observations have also been reported by Smahhi et al. [11] for an $x=0.3$ lithium silicoaluminate $\text{Li}_{4.3}\text{Al}_{0.3}\text{Si}_{0.7}\text{O}_4$ powder. Dehydration occurs at 100 °C, leading to a mixture of unreacted SiO_2 and LiOH below 400 °C. The two endothermic peaks at $T=422$ and 467 °C, respectively, can be attributed to the decomposition of LiOH which melts at 475 °C [15]. The second stage consisted of three successive thermal treatments of about 10 h each at 800 °C, with alternating intervals of cooling from 750 °C to room temperature and grinding to fine particles.

Several attempts have been made to synthesize pure compositions in the $\text{Li}_{4+x}\text{B}_x\text{Si}_{1-x}\text{O}_4$ solid solution by varying the firing temperature (670, 750 and 850 °C), by varying the firing times (up to 80 h), or by using different starting materials ($\text{LiOH}\cdot\text{H}_2\text{O}$, Li_2CO_3 , Li_4SiO_4). The major problem is the reaction of Li_2O

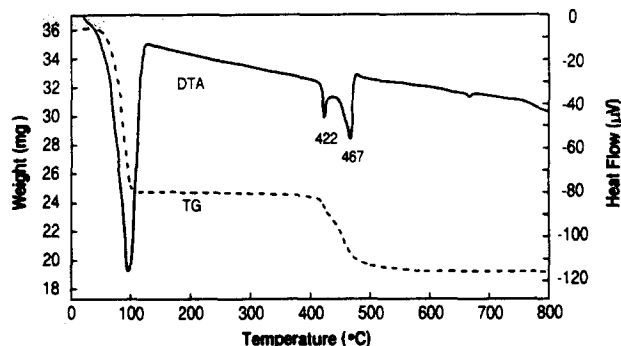


Fig. 1. Thermogravimetric (TG) and differential thermal analysis (DTA) curves of the dehydration of an initial mixture $4\text{LiOH}\cdot\text{H}_2\text{O} + \text{SiO}_2$. Firing up to 800 °C under ambient atmosphere. Sample mass = 36 mg. Heating rate = 10 °C min^{-1} .

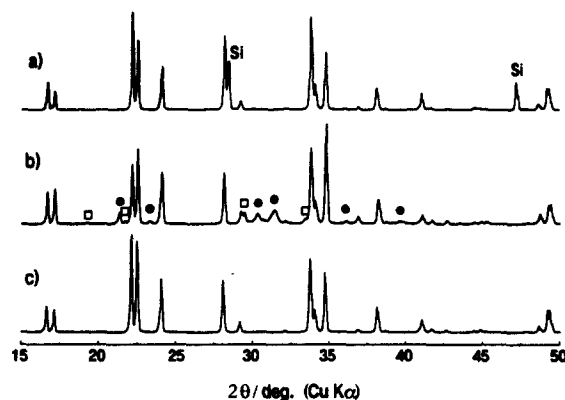


Fig. 2. X-ray diffraction patterns of: (a) $\text{Li}_{4.2}\text{B}_{0.2}\text{Si}_{0.8}\text{O}_4$; (b) initial composition $x=0.2$ fired at 670 °C, and (c) Li_4SiO_4 . Extra peaks: (□) Li_3BO_3 , and (●) $\text{Li}_{2+x}\text{C}_{1-x}\text{B}_x\text{O}_3$.

with the CO_2 of the atmosphere, which leads to the formation of Li_2CO_3 . At 670 °C, significant amounts of Li_3BO_3 , Li_2CO_3 and/or $\text{Li}_{2+x}\text{C}_{1-x}\text{B}_x\text{O}_3$ compositions are detected (Fig. 2), the quantity of which is clearly related to the value of x in the starting mixture. The solubility of boron in the Li_4SiO_4 structure is higher at 750 °C, as demonstrated by the absence of Li_3BO_3 , but Li_2CO_3 and/or $\text{Li}_{2+x}\text{C}_{1-x}\text{B}_x\text{O}_3$ are still detected. At 850 °C, we obtained $\text{Li}_{4+x}\text{B}_x\text{Si}_{1-x}\text{O}_4$ compositions exempt from Li_3BO_3 or Li_2CO_3 , up to $x=0.2$ only, by using Li_4SiO_4 , $\text{LiOH}\cdot\text{H}_2\text{O}$ and H_3BO_3 as starting materials. Prolonged thermal treatments were unsuccessful and led to the formation of Li_2SiO_3 due to an excessive volatilization of Li_2O .

3.2. Synthesis in a CO_2 -free atmosphere

A second series of experiments was carried out by firing the mixtures at 850 °C in an argon atmosphere. H_3BO_3 , SiO_2 and $\text{LiOH}\cdot\text{H}_2\text{O}$ (A-method) or Li_2CO_3 (B-method) were used as starting materials for initial compositions with $0 \leq x \leq 0.7$. Under these conditions, there is no Li_2CO_3 impurity formation. Thus, depending on the firing time, the major extra phases coexisting

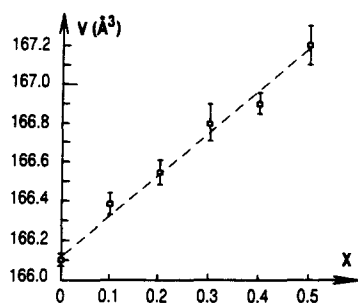


Fig. 3. Volume of the unit cell as a function of x in the $\text{Li}_{4+x}\text{B}_x\text{Si}_{1-x}\text{O}_4$ solid solution.

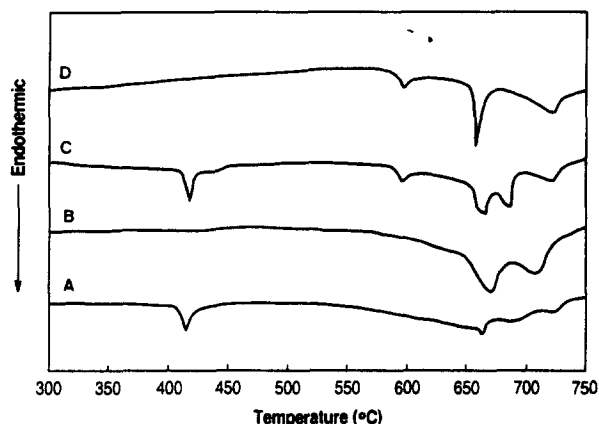


Fig. 4. DTA curves recorded between 300 and 750 °C for: (A) $\text{Li}_{4.3}\text{B}_{0.3}\text{Si}_{0.7}\text{O}_4$ obtained from $\text{LiOH}\cdot\text{H}_2\text{O}$; (B) $\text{Li}_{4.3}\text{B}_{0.3}\text{Si}_{0.7}\text{O}_4$ obtained from Li_2CO_3 ; (C) $\text{Li}_4\text{SiO}_4 + 3\% \text{LiOH}$, and (D) pure Li_4SiO_4 .

with the solid-solution compounds are Li_3BO_3 and Li_2SiO_3 . After a thermal treatment of 10 h at 850 °C, initial mixtures of $0 \leq x \leq 0.5$ lead to solids which, from XRD patterns, appear to be pure solid-solution compounds. A systematic shift towards the small angles of the XRD peaks is observed as x is increased, which corresponds directly with the evolution of the unit-cell volume with x as shown in Fig. 3. For starting compositions of $x > 0.5$, the solid solution is, without exception, accompanied with significant amounts of Li_3BO_3 and/or Li_2SiO_3 . From this observation, we conclude that the solubility limit of boron in the LiSiO_4 -based solid solution is $x \leq 0.5$.

4. Thermal analysis

DTA experiments were performed on Li_4SiO_4 and $\text{Li}_{4+x}\text{B}_x\text{Si}_{1-x}\text{O}_4$ compositions in an ambient atmosphere. A selection of the obtained data is presented in Fig. 4. The thermal evolution of pure Li_4SiO_4 (curve (D)) is characterized by three reversible peaks at $T = 597$, 657 and 720 °C, with a small hysteresis upon cooling. This agrees with the previous results reported by West and Glasser [16] who suggested the existence of a polymorphic transition between a 'low-temperature' and a 'high-temperature' form of Li_4SiO_4 . Fig. 4 also shows

the thermal evolution of two $\text{Li}_{4+x}\text{B}_x\text{Si}_{1-x}\text{O}_4$ compositions where $x = 0.3$, prepared using the A- and B-methods described above. For both samples, small thermal effects are also detected between 650 and 730 °C but they are either more diffuse or smaller than those for pure Li_4SiO_4 . An additional peak at $T = 418$ °C is observed for the A-samples (prepared via $\text{LiOH}\cdot\text{H}_2\text{O}$), which we attribute to the presence of unreacted LiOH within the material. A similar peak can be observed on the curve (C) obtained from pure Li_4SiO_4 to which small amounts of LiOH (3%) were deliberately added. These observations are of importance, as the presence of LiOH impurity phase was earlier reported to enhance notably the ionic conductivity of $\text{Li}_{4+x}\text{Al}_x\text{Si}_{1-x}\text{O}_4$ [11] or Li_5AlO_4 [17] materials. B-samples prepared in an argon atmosphere do not show such thermal effects, but it is noteworthy that additional firing in an ambient atmosphere or exposure to the moisture in the air also results in LiOH formation.

5. Lithium insertion into the Li_4SiO_4 structure

The crystal structure of the low-temperature form of Li_4SiO_4 has been previously described by three different research groups [12-14]. Li_4SiO_4 crystallizes in the monoclinic system, space group $P2_1/m$ and consists of isolated SiO_4^{4-} tetrahedra and Li^+ ions, which occupy the interstitial space. It was first described by Vollenkle et al. [12] as a disordered structure at room temperature in which the Li^+ ions partially occupy six independent crystallographic sites. On the Li(1) to Li(4) sites, the Li^+ ions are tetrahedrally coordinated by oxygen atoms while they are five and six-coordinated on Li(5) and Li(6) sites, respectively. Three of the lithium sites are in general position $4f$ Li(1), Li(4) and Li(5)). The others are in special positions $2e$ (Li(2), Li(3) and Li(6)). Tranqui et al. [13] demonstrated that Li_4SiO_4 can also exist in an ordered form with a supercell seven times larger due to the necessity of an ordered distribution of the Li^+ ions. The ratio 'occupied sites/total available sites' for each set of lithium sites are given in Table 1, along with the distances between neighboring lithium positions in the description by Baur and Ohta [14]. The importance of this lies in the fact that neighboring lithium positions are very close to each other (from 1.02 to 2.06 Å) and, thus, cannot be totally simultaneously occupied (Fig. 5). Therefore, for each of these lithium-pairs, the summation of the occupancy rates should not exceed unity. This allows us to calculate the maximum number of extra Li^+ ions which can be incorporated into the Li_4SiO_4 structure. It is obvious then, that the maximum occupancy rate τ_{max} of both Li(4) and Li(5) sites is equal to 0.5, because of the proximity of two symmetrically related sites (Li(4)-Li(4')) or Li(5)-Li(5')). Assuming that these occupancies are effectively equal to 0.5, this, for the same reason, leads

Table 1
Occupancy factors and distances between neighboring lithium sites

Lithium site	CN ^a	Position	τ^b [13]	Lithium–lithium distances (Å) [14]	Sum τ	
Li(1)	4	4f	4/7	Li(4)	1.18	1
				Li(5)	1.64	6/7
				Li(6)	1.95	1
				Li(6)	2.05	1
Li(2)	4	2e	4/7	Li(3)	1.16	1
				Li(4)	1.85	1
Li(3)	4	2e	3/7	Li(2)	1.16	1
				Li(5)	1.65	5/7
				Li(6)	2.01	6/7
Li(4)	4	4f	3/7	Li(1)	1.18	1
				Li(2)	1.85	1
				Li(4)	1.95	6/7
Li(5)	5	4f	2/7	Li(1)	1.64	6/7
				Li(3)	1.65	5/7
				Li(5)	1.02	4/7
Li(6)	6	2e	3/7	Li(1)	1.95	1
				Li(1)	2.06	1
				Li(3)	2.01	6/7

^a CN = coordination number.

^b τ = occupied sites/available sites in the superstructure description [13].

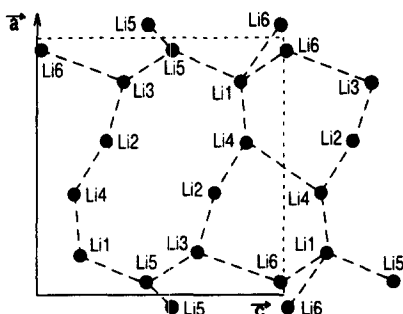


Fig. 5. Partial representation of the lithium sites positions in Li_4SiO_4 [12]. Distances between neighboring lithium sites are given in Table 1.

to the conclusion that $\tau_{\max} = 0.5$ for Li(1), Li(2) and Li(3). Moreover, if $\tau(\text{Li}(1)) = 0.5$, $\tau_{\max}(\text{Li}(6))$ is also equal to 0.5. The maximum amount of Li^+ ions can, therefore, be calculated by also taking into account the multiplicity of each site. If $\tau = 0.5$ for each of them, this supposes 9 Li^+ ions per unit cell, thus, 4.5 Li^+ ions per XO_4 tetrahedra. This suggests that $\text{Li}_{4.5}\text{B}_{0.5}\text{Si}_{0.5}\text{O}_4$ is the maximum composition, above which Li^+ insertion cannot occur without a modification of the Li_4SiO_4 -based structure.

6. Conclusions

This study was first commenced in order to provide a better understanding of the sharp increase in the

ionic conductivity of Li_4SiO_4 which occurs when silicon is substituted with trivalent cations M^{3+} ($\text{M} = \text{Al}, \text{Ga}, \text{B}$), leading to compounds of the general formula $\text{Li}_{4+x}\text{M}_x\text{Si}_{1-x}\text{O}_4$. From this work, devoted to the boron-substituted compounds, it appears that the atmosphere in which the synthesis is carried out has a major influence on Li_2CO_3 and/or LiOH impurities formation. The presence of these extra phases may have a major role in enhancing the ionic conductivity, as was previously demonstrated by Smaïhi et al. [11] for $\text{Li}_{4+x}\text{Al}_x\text{Si}_{1-x}\text{O}_4$ and Johnson et al. [17] for Li_5AlO_4 materials. The Li insertion mechanism is also considered here from which we demonstrate that there is a theoretical upper limit of $x = 0.5$ above which Li^+ ions cannot be introduced without a modification of the Li_4SiO_4 -based structure. Conductivity measurements and crystal structure determinations of various compositions are now under investigation and will be reported in a forthcoming paper.

Acknowledgement

C. Masquelier thanks the STA, Japan, for providing a fellowship.

References

- [1] W. Gratzler, H. Bittner, H. Nowotny and K. Seifert, *Z. Kristallogr.*, **133** (1971) 260.
- [2] A.R. West, *J. Appl. Electrochem.*, **3** (1973) 327.
- [3] K. Jackowska and A.R. West, *J. Mater. Science*, **18** (1983) 2380–2384.
- [4] P. Quintana and A.R. West, *Br. Ceram. Trans. J.*, **88** (1989) 17–20.
- [5] R.D. Shannon, B.E. Taylor, A.D. English and T. Berzins, *Electrochim. Acta*, **22** (1977) 783–796.
- [6] P. Quintana, F. Velasco and A.R. West, *Solid State Ionics*, **34** (1989) 149–155.
- [7] Y. Saito, K. Ado, T. Asai, H. Kageyama and O. Nakamura, *Solid State Ionics*, **47** (1991) 149–154.
- [8] R.I. Smith and A.R. West, *J. Solid State Chem.*, **88** (1990) 564–570.
- [9] R.I. Smith and A.R. West, *Proc. Symp. Materials Research Society*, Vol. 210, Materials Research Society, Pittsburgh, PA, 1991.
- [10] Y. Saito, T. Asai, K. Ado, H. Kageyama and O. Nakamura, *Solid State Ionics*, **40/41** (1990) 34–37.
- [11] M. Smaïhi, D. Petit, J.P. Korb and J.P. Boilot, *J. Solid State Chem.*, **94** (1991) 260–273.
- [12] H. Vollenkle, A. Wittmann and H. Nowotny, *Monatsh. Chem.*, **99** (1968) 1360–1371.
- [13] D. Tranqui, R.D. Shannon and H.Y. Chen, *Acta Crystallogr. Sect. B*, **35** (1979) 2479–2487.
- [14] W.H. Baur and T. Ohta, *J. Solid State Chem.*, **44** (1982) 50–59.
- [15] O.G. Perfil'eva and N.A. Reshetnikov, *Russ. J. Inorg. Chem.*, **9** (1964) 1405–1407.
- [16] A.R. West and F.P. Glasser, *J. Mater. Science*, **5** (1970) 676–688.
- [17] R.T. Johnson, R.M. Biefeld and J.D. Deck, *Mater. Res. Bull.*, **12** (1977) 577–587.